AIP | Applied Physics Letters

Ultralow-power all-optical tunable double plasmon-induced transparencies in nonlinear metamaterials

Yu Zhu, Xiaoyong Hu, Hong Yang, and Qihuang Gong

Citation: Applied Physics Letters **104**, 211108 (2014); doi: 10.1063/1.4881056
View online: http://dx.doi.org/10.1063/1.4881056
View Table of Contents: http://scitation.aip.org/content/aip/journal/apl/104/21?ver=pdfcov
Published by the AIP Publishing

Ultralow-power all-optical tunable double plasmon-induced transparencies in nonlinear metamaterials

Yu Zhu,[1] Xiaoyong Hu,[1,2,a)] Hong Yang,[1] and Qihuang Gong[1,2,a)]
[1]*State Key Laboratory for Mesoscopic Physics and Department of Physics, Peking University, Beijing 100871, People's Republic of China*
[2]*Collaborative Innovation Center of Quantum Matter, Beijing 100871, People's Republic of China*

(Received 24 March 2014; accepted 18 May 2014; published online 30 May 2014)

An all-optical tunable double plasmon-induced transparency is realized in a photonic metamaterial coated on the surface of a nanocomposite layer made of polycrystalline indium-tin oxide doped with gold nanoparticles. The local-field effect, quantum confinement effect, and hot-electron injection ensure a large optical nonlinearity for the nanocomposite. A shift of 120 nm in the central wavelength of transparency windows is reached under excitation with a weak pump laser with an intensity of 21 kW/cm^2. Compared with previous reports, the threshold pump intensity is reduced by five orders of magnitude, while an ultrafast response time of 34.9 ps is maintained. © *2014 AIP Publishing LLC*. [http://dx.doi.org/10.1063/1.4881056]

Plasmon-induced transparency (PIT) in photonic metamaterials has great potential applications in the field of integrated photonic devices.[1] The basic idea is to use destructive interference coupling between super- and sub-radiant plasmonic modes provided by meta-molecules.[2,3] Various meta-molecular configurations, including two-gap split ring resonator (SRR),[4] a metallic nanowire side-coupled two SRRs,[5] metallic nanorod octomer,[6] and metallic nano-cuboid trimer,[7,8] have been adopted. Only one transparency window was obtained using these configurations. Many integrated photonic devices require multiple transparency windows.[9] The fundamental realization method is to construct the meta-molecule by using multiple bright and dark meta-atoms, including the bright-dark-bright, bright-bright-dark, or dark-bright-dark configurations.[10,11] In 2011, Liu *et al.* reported double transparency windows in a photonic metamaterial whose meta-molecule was composed of a gold nanorod (acting as bright meta-atom) side coupled two gold nanorod pairs (acting as two dark meta-atoms).[12] Recently, Yin *et al.* also realized double transparency windows in a terahertz metamaterial whose meta-molecule consisted of a gold nano-strip (acting as bright meta-atom) side coupled two gold SRR pairs (acting as two dark meta-atoms).[13] Ultrafast and actively tunable multiple transparency windows are urgently needed in integrated photonic chips based on metamaterials.[14]

Here, we report an ultrafast and ultralow-power all-optical tunable double PITs in a photonic metamaterial coated on the surface of a nonlinear nanocomposite film made of high-conductivity polycrystalline indium-tin oxide (ITO) doped with gold nanoparticles (nano-Au:polycrystalline-ITO). The meta-molecule (Fig. 1(a)) consisted of one dark meta-atom side-coupled two bright meta-atoms. Owing to the destructive interference coupling between two superradiant modes and one subradiant mode, double transparency windows were obtained.[12] The nanocomposite nano-Au:polycrystalline-ITO could provide a very large third-order nonlinear susceptibility due to three nonlinearity enhancement factors, i.e., quantum confinement effect provided by nanoscale ITO crystal grains,[8] hot-electron injection from gold nanostructures to polycrystalline ITO under excitation with a pump laser,[15] and local-field effect originating from the nonuniform electric-field distribution of incident laser between two constituents of the nanocomposite.[16] An ultrafast response time of 34.9 ps was maintained simultaneously.

The photonic metamaterial was fabricated by using a laser molecular beam epitaxy growth system (Model LMBE 450, SKY Company, China) and a focused ion-beam etching system (Model DB 235, FEI Company, USA). The fabrication process was detailed in Ref. 8. The doping concentration was 7% for gold nanoparticles. The meta-molecule (Fig. 1(b)) was composed of a vertical gold nanocuboid pair (acting as a dark meta-atom) side-coupled a long gold nanocuboid (acting as a bright meta-atom) and a horizontal gold nanocuboid pair (acting as another bright meta-atom) deposited on a 180-nm-thick nanocomposite nano-Au:polycrystalline-ITO layer. The length, width, and height were 300, 100, and 60 nm for the long gold nanocuboid, respectively. Two nanocuboid pairs were constructed using four identical short gold cuboids with the length of 260 nm, width of 100 nm, and height of 60 nm. The distance between two short gold cuboids forming the horizontal nanocuboid pair was 100 nm, while that was 60 nm for the vertical one. The distance between the bright meta-atom and the dark meta-atom was 50 nm. The photonic metamaterial (Fig. 1(c)) was composed of periodic arrays of square lattice of meta-molecules. The lattice constant was 700 nm. The patterned area was about 100 μm × 100 μm. The top-view SEM image of a 180-nm-thick nanocomposite layer is shown in Fig. 1(d). The ITO takes on the polycrystalline crystal configuration constructed from nanoscale crystal grains with an average size of 120 nm. The yellow areas in Fig. 1(e) were gold nanoparticles, which have an average size of about 70 nm. Figure 1(f) shows the measured transmission and reflectance spectra of a 180-nm-thick nanocomposite film by using a Fourier transform infrared spectrometer system (Model Magna-IR 750, Nicolet Company, USA). The cross point of the transmission and reflectance curves was localized at

a)Authors to whom correspondence should be addressed. Electronic addresses: xiaoyonghu@pku.edu.cn and qhgong@pku.edu.cn

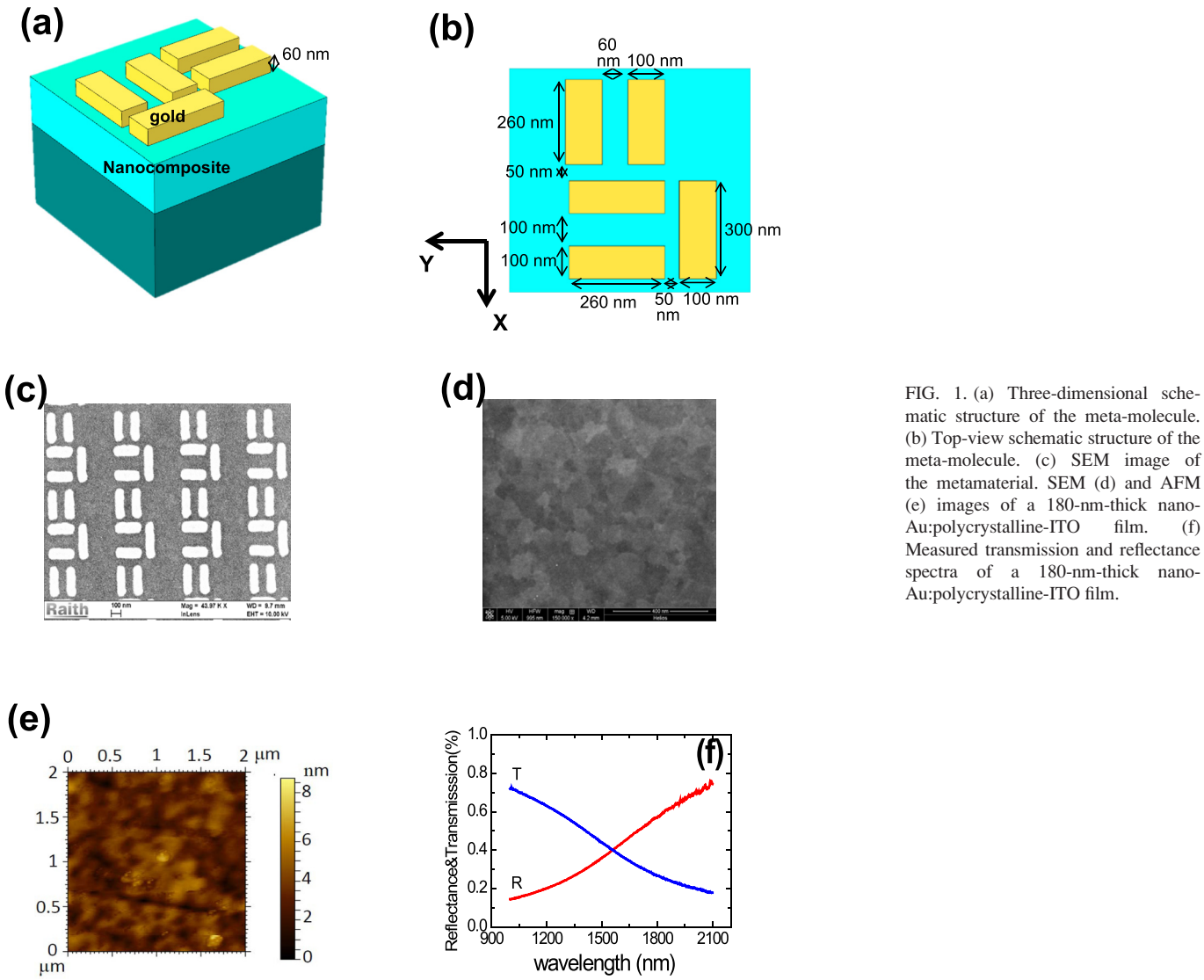

FIG. 1. (a) Three-dimensional schematic structure of the meta-molecule. (b) Top-view schematic structure of the meta-molecule. (c) SEM image of the metamaterial. SEM (d) and AFM (e) images of a 180-nm-thick nano-Au:polycrystalline-ITO film. (f) Measured transmission and reflectance spectra of a 180-nm-thick nano-Au:polycrystalline-ITO film.

1560 nm, which ensures the perfect dielectric response of the nanocomposite for the measurements in the wavelength range less than 1560 nm.[17]

To study the double PITs, we measured the linear transmission spectrum of the photonic metamaterial by using a micro-spectrum measurement system (detailed in Ref. 8). The measured transmission was normalized with respect to a pure 180-nm-thick nano-Au: polycrystalline-ITO film.[18] The measured linear transmission spectrum for the TM polarization incidence case, i.e., the electric-field vector of the incident light was parallel to X axis (as shown in Fig. 1(b)), is plotted in Fig. 2(a). Two transmission peaks appeared in the wide transmission forbidden band, as indicated by the Gaussian fitted results, which implies the formation of double PITs. The central wavelength was 1233 nm for the transparency window in the short-wavelength direction, and 1348 nm for that in the long-wavelength direction, which are in agreement with the calculated ones (Fig. 2(b)) by using the finite element method.[18] In our calculations, the frequency-dependent dielectric constant of gold was obtained from Ref. 19. The refractive index of air was set to be 1. The effective refractive index of the nanocomposite was set to be 1.7. The measured peak transmission was 27% for the transparency window in the short-wavelength direction and 42% for that in the long-wavelength direction, which is smaller than the calculated one, i.e., 33% for the transparency window in the short-wavelength direction and 60% for that in the long-wavelength direction. The reason lies in that the imperfectly etched structure of gold cuboids destroyed perfect plasmonic resonances properties. To confirm the physical mechanism of the double PITs, we calculated, using the finite element method, the electric-field distribution of the meta-molecule for the TM polarization incidence case at wavelengths of 1117, 1233, 1250, 1348, and 1430 nm. The electric-field distributions at 1117, 1250, or 1430 nm (all located at transmission minimum) were mainly confined around the end facets of the long gold nanocuboid or one nanocuboid of the horizontal nanocuboid pair, i.e., taking on the configuration of a composite dipole plasmonic resonance mode (acting as the superradiant mode), as shown in Figs. 2(c), 2(e), and 2(g), respectively. The electric-field distribution (Fig. 2(d)) at 1233 nm (located at the center of the transparency window in the short wavelength direction) was mainly confined around the end facets of the vertical nanocuboid pair and the long gold nanocuboid. The vertical nanocuboid pair provided a quadrupole plasmonic resonance mode (acting as the subradiant mode). This indicates that the transparency window centered at

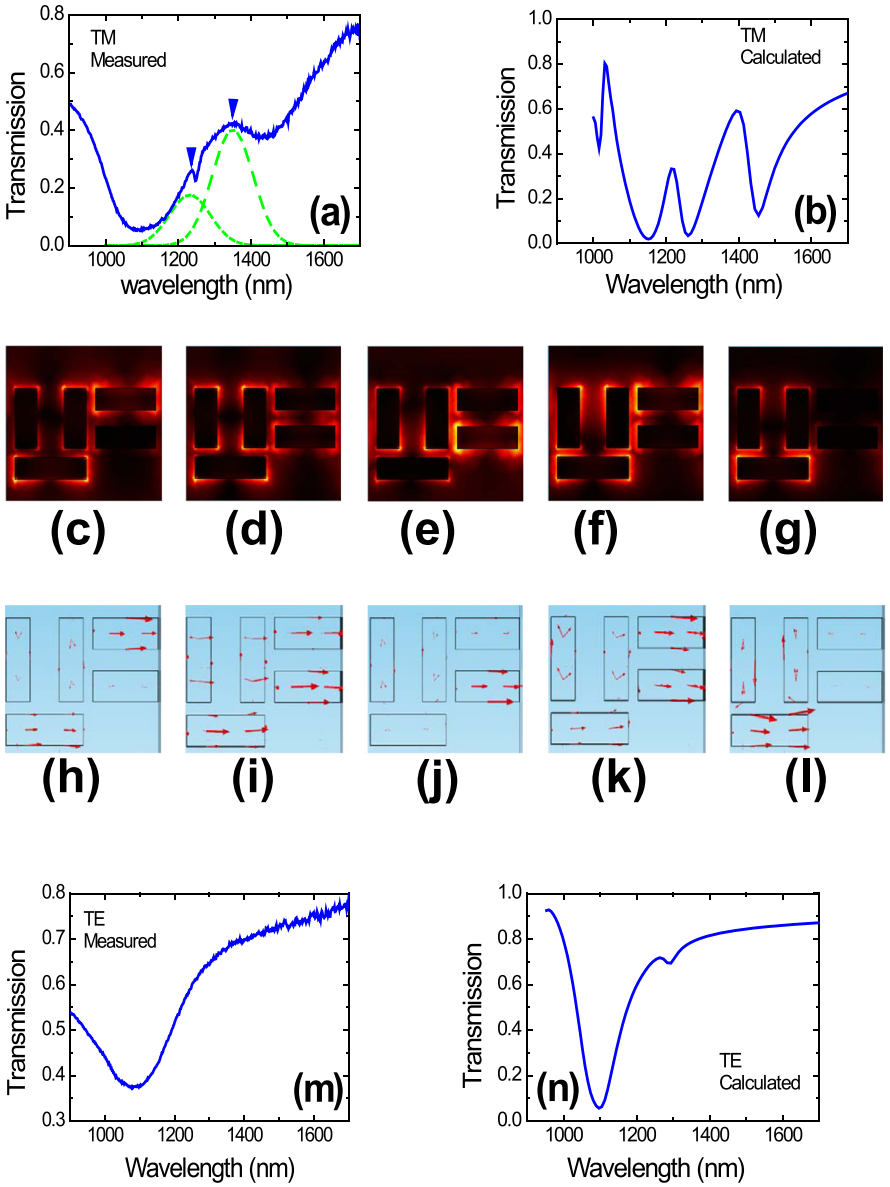

FIG. 2. Measured (a) and calculated (b) transmission spectra of the metamaterial for the TM polarization incidence case. The dashed lines are Gaussian fitted peak. The arrows indicate two transparency window peaks. Calculated electric-field distribution of the meta-molecule for the TM polarization incidence case when the incident light wavelength was 1117 nm (c), 1233 nm (d), 1250 nm (e), 1348 nm (f), 1430 nm (g). Calculated electric-current distributions on the surface of meta-molecule for the TM polarization incidence case when the incident light wavelength was 1117 nm (h), 1233 nm (i), 1250 nm (j), 1348 nm (k), 1430 nm (l). Measured (m) and calculated (n) transmission spectra of the metamaterial for the TE polarization incidence case.

1233 nm was formed by the destructive coupling between the superradiant mode provided by the long gold nanocuboid and the subradiant mode provided by the vertical nanocuboid pair. The electric-field distribution (Fig. 2(f)) at 1348 nm (located at the center of the transparency window in the long-wavelength direction) was mainly confined around the end facets of the vertical and horizontal nanocuboid pairs. This shows that the transparency window centered at 1348 nm was formed by the destructive interference coupling between the subradiant plasmonic mode provided by the vertical nanocuboid pair and the superradiant plasmonic mode provided by the horizontal nanocuboid pair. This was also confirmed by the calculated electric-current distributions on the surface of meta-molecule by using the finite element method, as shown in Figs. 2(h)–2(l). To further confirm the double PITs, we measured the linear transmission spectrum (Fig. 2(m)) of the photonic metamaterial for the TE polarization incidence case, i.e., the electric-field vector of the incident light was parallel to Y axis. Only a transmission dip centered at 1100 nm appeared in the transmission spectrum, which is in agreement with the calculated one (Fig. 2(n)) by using the finite element method. This indicates that the meta-molecule acts as a composite dipole plasmonic resonant antenna for the TE polarization incidence case.

To study the all-optical tunability, we measured the transmission change (Fig. 3(a)) of the 1500 nm probe laser as a function of the time delay between the pump and the probe pulses by using the femtosecond pump and probe method (detailed in Ref. 8). A 35-fs, 1-kHz beam from a femtosecond optical parameter amplifier system (Model Opera Solo, Coherent Company, USA) was used as light source. The wavelength was 1500 nm for both the pump and probe lights. The intensity was less than 1 kW/cm^2 for the probe light and 21 kW/cm^2 for the pump light. The measured signal curve showed a fast rise followed by a slow drop. The wavelength of the probe light was located at a transmission minimum, as shown in Fig. 2(a). The transmission of the probe light maintained the minimum value, 37%, in the temporal sequence where the pump pulse was far away from the probe pulse. When the pump and probe pulses overlapped temporally, the transmission of the probe light increased. According to the third-order nonlinear optical Kerr effect (OKE), the effective index n of the nanocomposite nano-Au:polycrystalline-ITO can be calculated by[20]

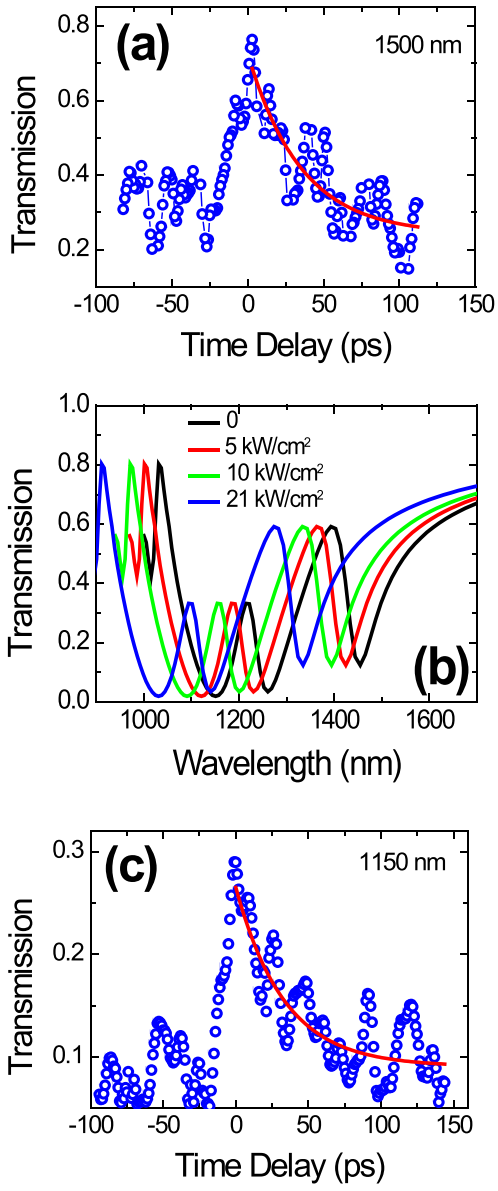

FIG. 3. (a) Measured transmission change of a 1500 nm probe laser as the function of a time delay between the pump and probe pulses by using the femtosecond pump and probe method. (b) Calculated transmission spectra of the metamaterial with different pump intensity. (c) Measured transmission change of a 1150 nm probe laser as the function of a time delay between the pump and probe pulses by using the femtosecond pump and probe method. The red thick line is the exponential fit to the data.

$$n = n_0 + n_2 I = n_0 + \frac{3\mathrm{Re}\chi^{(3)}}{4\varepsilon_0 c n_0^2} I, \tag{1}$$

where n_0, n_2, and $\mathrm{Re}\chi^{(3)}$ are effective linear and nonlinear refractive index, and the real part of the third-order nonlinear susceptibility of the nanocomposite; I is the pump intensity; ε_0 is the permittivity of a vacuum; and c is the light velocity in a vacuum. The nanocomposite nano-Au:polycrystalline-ITO has a negative value of nonlinear refractive index n_2, which makes the effective refractive index of the nanocomposite decrease under excitation with a pump light. The wavelength of the plasmonic resonance modes provided by a plasmonic microstructure was influenced tremendously by the refractive index of the ambient dielectric material.[21] A blue-shift in the resonant wavelength of the plasmonic modes can be obtained with a reduction in the refractive index of the ambient dielectric material.[22] As a result, two transparency windows shift in the short-wavelength direction and the transmission of the probe light increases. The maximum transmission of the probe light was 79% at the zero time delay. The operating pump intensity, 21 kW/cm^2, was reduced by five orders of magnitude compared with previously reports.[2–9,14] According to the Maxwell Garnett theory, the effective third-order nonlinear susceptibility $\chi^{(3)}$ of the nanocomposite nano-Au:polycrystalline-ITO can be written as[23]

$$\chi^{(3)} \approx (1-p)\left(\frac{\varepsilon_{\mathrm{eff}} + 2\varepsilon_h}{3\varepsilon_h}\right)^2 \left|\frac{\varepsilon_{\mathrm{eff}} + 2\varepsilon_h}{3\varepsilon_h}\right|^2 \chi_h^{(3)} + 3p\left(\frac{\varepsilon_{\mathrm{eff}} + 2\varepsilon_h}{\varepsilon_m + 2\varepsilon_h}\right)^2 \left|\frac{\varepsilon_{\mathrm{eff}} + 2\varepsilon_h}{\varepsilon_m + 2\varepsilon_h}\right|^2 \chi_m^{(3)}, \tag{2}$$

where p is the volume fraction of gold nanoparticles, $\varepsilon_{\mathrm{eff}}$, ε_h, and ε_m are the permittivity of the nanocomposite, polycrystalline ITO, and gold nanoparticles, respectively. $\chi_h^{(3)}$ and $\chi_m^{(3)}$ are third-order nonlinear susceptibility of polycrystalline ITO and gold nanoparticles, respectively. $\frac{\varepsilon_{\mathrm{eff}}+2\varepsilon_h}{3\varepsilon_h}$ and $\frac{\varepsilon_{\mathrm{eff}}+2\varepsilon_h}{\varepsilon_m+2\varepsilon_h}$ are local-field enhancement factors, originating from the nonuniform field distribution of incident light between polycrystalline ITO and gold nanoparticles, which devotes to the nonlinearity enhancement of the nanocomposite.[16] The nanoscale crystal grains in polycrystalline ITO could provide strong quantum confinement effect, which also contributes to the nonlinearity enhancement of the nanocomposite.[8] Moreover, the hot-electron injection from gold microstructures to polycrystalline ITO under excitation with a pump laser also dedicates to the nonlinearity enhancement of the nanocomposite.[15] Therefore, the nanocomposite provides a very large third-order nonlinear susceptibility, which results in an ultralow threshold pump intensity. To confirm the measured results, we calculated using the finite element method the transmission spectrum (Fig. 3(b)) of the photonic metamaterial under excitation with a pump light. The central wavelengths of two transparency windows shifted in the short-wavelength direction under excitation with a pump light. When the pump intensity increased from zero to 21 kW/cm^2, the central wavelength of the transparency window in the short-wavelength direction shifted from 1233 to 1101 nm, while that in the long-wavelength direction shifted from 1348 to 1273 nm. A shift of 120 nm in the central wavelength of transparency windows was obtained. To further confirm the all-optical tunability, we measured the closed-aperture Z-scan curve (Fig. 4(a)) of a 180-nm-thick nano-Au:polycrystalline-ITO film.[8] A 1500-nm, 35-fs laser beam (with repetition rate 1 kHz) was used as the light source. The experimental setup was detailed in Ref. 8. The nonlinear refractive index of the nanocomposite was measured to be -1.02×10^{-8} cm^2/W, which is six orders of magnitude larger than that of silicon in the optical communication range, -3.2×10^{-14} cm^2/W.[23]

The dynamical process of the transmission changes in Fig. 3(a) indicates the time response properties of the all-optical tunability. The fast rise is attributed to the formation of nonequilibrium electrons in gold and free carriers in polycrystalline ITO.[8] The red thick line was exponentially fitted results of the drop curve. The characteristic time was fitted to be 34.9 ps. For gold nanoparticles, the electron-electron

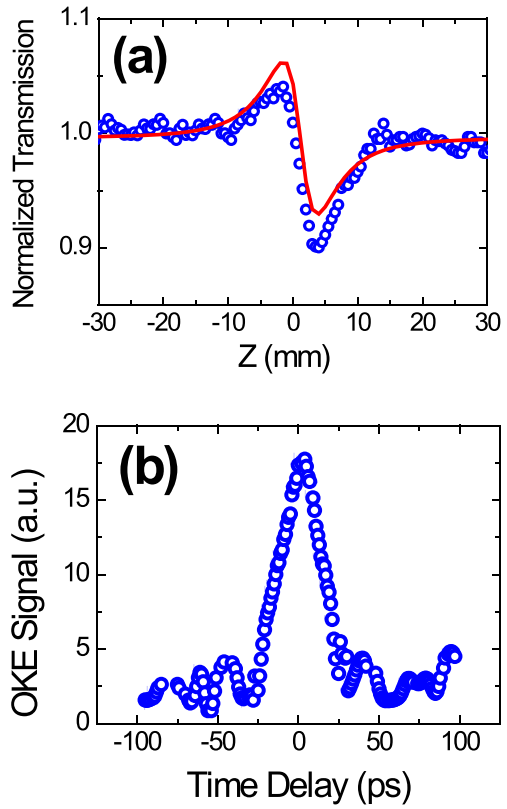

FIG. 4. (a) Measured closed-aperture Z-scan curve of a 180-nm-thick nano-Au:polycrystalline-ITO film. The red thick line is the exponential to the data. (b) Measured OKE response of a 180-nm-thick nano-Au:polycrystalline-ITO film.

scattering redistributes the energy in the conduction electrons with a characteristic time of less than 500 fs.[24] Subsequently, the energy is transferred to the lattice by electron-phonon interactions on a time scale of 2–3 ps.[25] Finally, the phonon-phonon interactions redistribute the energy with a characteristic time of 24 ps.[26] The hot-electron injection from gold nanocuboids to polycrystalline ITO only responses on a time scale of subpicosecond order.[15] The fast carrier recombination at lattice defects of nanoscale crystal grains of polycrystalline ITO ensures an ultrafast response time.[27] To confirm the time response of the nanocomposite, we measured the OKE responses (Fig. 4(b)) of a 180-nm-thick nano-Au:polycrystalline-ITO film by using a femtosecond optical Kerr gate method.[28] A 1500-nm, 35-fs laser beam (with repetition rate 1 kHz) was used as the light source. The half width of the signal envelope was in proximity to 35 ps. We also measured the transmission change (Fig. 3(c)) of the 1150 nm probe laser as a function of the time delay between the pump and the probe pulses. The transmission of the probe light maintained the minimum value, 7%, in the temporal sequence where the pump pulse was far away from the probe pulse. The maximum transmission of the probe light was 27% at the zero time delay, which are in agreement with the calculations (Fig. 3(b)). The red thick line in Fig. 3(c) was exponentially fitted results of the drop curve. The characteristic time was fitted to be 34.9 ps. This confirms the all-optical nonlinear control of the double-PIT. We could not obtain the entire transmission spectrum under pump light due to the intrinsic limitations of the femtosecond pump and probe method. The remarkable advantage of all-optical control lies in the ultrafast response time.

In summary, we have realized all-optical tunable double PIT in a photonic metamaterial coated on a nano-Au:polycrystalline-ITO layer. Under excitation with a weak pump laser of 21 kW/cm^2, a shift of 120 nm in the central wavelength of transparency windows was realized. An ultrafast response time of 34.9 ps was maintained simultaneously. This opens up the possibility for the realization of low-power integrated photonic devices and quantum solid chips based on photonic metamaterials.

This work was supported by the 973 Program of China under Grant Nos. 2013CB328704 and 2014CB921003, the National Natural Science Foundation of China under Grant Nos. 11225417, 11134001, 11121091, and 90921008, and the Program for NCET in University.

[1]N. Paapasimakis, Y. H. Fu, V. A. Fedotov, S. L. Prosvirnin, D. P. Tsai, and N. I. Zheludev, Appl. Phys. Lett. **94**, 211902 (2009).
[2]C. Kurter, P. Tassin, L. Zhang, T. Koschny, A. P. Zhuravel, A. V. Ustinov, S. M. Anlage, and C. M. Soukoulis, Phys. Rev. Lett. **107**, 043901 (2011).
[3]N. Papasimakis, V. A. Fedotov, N. I. Zheludev, and S. L. Prosvirnin, Phys. Rev. Lett. **101**, 253903 (2008).
[4]R. Singh, I. A. I. Ainaib, Y. P. Yang, D. R. Chowdhury, W. Cao, C. Rockstuhl, T. Ozaki, R. Morandotti, and W. L. Zhang, Appl. Phys. Lett. **99**, 201107 (2011).
[5]X. J. Liu, J. Q. Gu, R. Singh, Y. F. Ma, J. Zhu, Z. Tian, M. X. He, J. G. Han, and W. L. Zhang, Appl. Phys. Lett. **100**, 131101 (2012).
[6]X. Y. Duan, S. Q. Chen, H. F. Yang, H. Cheng, J. J. Li, W. W. Liu, C. Z. Gu, and J. G. Tian, Appl. Phys. Lett. **101**, 143105 (2012).
[7]S. Zhang, D. A. Genov, Y. Wang, M. Liu, and X. Zhang, Phys. Rev. Lett. **101**, 047401 (2008).
[8]Y. Zhu, X. Y. Hu, Y. L. Fu, H. Yang, and Q. H. Gong, Sci. Rep. **3**, 2338 (2013).
[9]N. Liu, L. Langguth, T. Weiss, J. Kastel, M. Fleischhauer, T. Pfau, and H. Giessen, Nature Mater. **8**, 758 (2009).
[10]X. J. He, J. M. Wang, X. H. Tian, J. X. Jiang, and Z. X. Geng, Opt. Commun. **291**, 371 (2013).
[11]X. R. Su, Z. S. Zhang, L. H. Zhang, Q. Q. Li, C. C. Chen, Z. J. Yang, and Q. Q. Wang, Appl. Phys. Lett. **96**, 043113 (2010).
[12]N. Liu, M. Hentschel, T. Weiss, A. P. Alivisatos, and H. Giessen, Science **332**, 1407 (2011).
[13]X. G. Yin, T. H. Feng, S. Yip, Z. X. Liang, A. Hui, J. C. Ho, and J. S. Li, Appl. Phys. Lett. **103**, 021115 (2013).
[14]J. Q. Gu, R. Singh, X. J. Liu, X. Q. Zhang, Y. F. Ma, S. Zhang, S. A. Maier, Z. Tian, A. K. Azad, H. T. Chen, A. J. Taylor, J. G. Han, and W. L. Zhang, Nat. Commun. **3**, 1151 (2012).
[15]D. Traviss, R. Bruck, B. Mills, M. Abb, and O. L. Muskens, Appl. Phys. Lett. **102**, 121112 (2013).
[16]G. L. Fischer, R. W. Boyd, R. J. Gehr, S. A. Jenekhe, J. A. Osaheni, J. E. Sipe, and L. A. W. Brophy, Phys. Rev. Lett. **74**, 1871 (1995).
[17]E. Shanti, V. Dutta, A. Banerjee, and K. L. Chopra, J. Appl. Phys. **51**, 6243 (1980).
[18]F. Zhang, X. Y. Hu, Y. Zhu, H. Yang, and Q. H. Gong, Appl. Phys. Lett. **103**, 191116 (2013).
[19]P. B. Johnson and R. W. Christy, Phys. Rev. B **6**, 4370 (1972).
[20]R. W. Boyd, *Nonlinear Optics* (Academic press Inc., San Diego, USA, 1992).
[21]B. Lukyanchuk, N. I. Zheludev, S. A. Maier, N. J. Halas, P. Nordlander, H. Giessen, and C. T. Chong, Nature Mater. **9**, 707 (2010).
[22]E. Hendry, P. J. Hale, J. Moger, and A. K. Savchenko, Phys. Rev. Lett. **105**, 097401 (2010).
[23]S. Sederberg and A. Y. Elezzabi, Appl. Phys. Lett. **102**, 011133 (2013).
[24]N. D. Fatti, C. Voisin, M. Achermann, S. Tzortzakis, D. Christofilos, and F. Vallee, Phys. Rev. B **61**, 16956 (2000).
[25]R. W. Schoenlein, W. Z. Lin, J. G. Fujimoto, and G. L. Eesley, Phys. Rev. Lett. **58**, 1680 (1987).
[26]J. Sasai and K. Hirao, J. Appl. Phys. **89**, 4548 (2001).
[27]M. D. Losego, A. Y. Efremenko, C. L. Rhodes, M. G. Cerruti, S. Franzen, and J. P. Maria, J. Appl. Phys. **106**, 024903 (2009).
[28]Y. Zhu, X. Y. Hu, Y. Y. Huang, H. Yang, and Q. H. Gong, Adv. Opt. Mater. **1**, 61 (2013).